

Singapore Management University

Institutional Knowledge at Singapore Management University

Research Collection School Of Computing and Information Systems

School of Computing and Information Systems

1-1993

Observation of B₀ decay to two charmless mesons

M. BATTLE

Manoj THULASIDAS

Singapore Management University, manojt@smu.edu.sg

Follow this and additional works at: https://ink.library.smu.edu.sg/sis_research



Part of the [Databases and Information Systems Commons](#), and the [Software Engineering Commons](#)

Citation

1

This Journal Article is brought to you for free and open access by the School of Computing and Information Systems at Institutional Knowledge at Singapore Management University. It has been accepted for inclusion in Research Collection School Of Computing and Information Systems by an authorized administrator of Institutional Knowledge at Singapore Management University. For more information, please email cherylds@smu.edu.sg.

Observation of B^0 Decay to Two Charmless Mesons

M. Battle,¹ J. Ernst,¹ H. Kroha,¹ Y. Kwon,¹ S. Roberts,¹ K. Sparks,¹ E. H. Thorndike,¹ C. H. Wang,¹ J. Dominick,² S. Sanghera,² V. Shelkov,² T. Skwarnicki,² R. Stroynowski,² I. Volobouev,² P. Zadorozhny,² M. Artuso,³ D. He,³ M. Goldberg,³ N. Horwitz,³ R. Kennett,³ G. C. Moneti,³ F. Muheim,³ Y. Mukhin,³ S. Playfer,³ Y. Rozen,³ S. Stone,³ M. Thulasidas,³ G. Vasseur,³ G. Zhu,³ J. Bartelt,⁴ S. E. Csorna,⁴ Z. Egyed,⁴ V. Jain,⁴ P. Sheldon,⁴ D. S. Akerib,⁵ B. Barish,⁵ M. Chadha,⁵ S. Chan,⁵ D. F. Cowen,⁵ G. Eigen,⁵ J. S. Miller,⁵ C. O'Grady,⁵ J. Urheim,⁵ A. J. Weinstein,⁵ D. Acosta,⁶ M. Athanas,⁶ G. Masek,⁶ H. Paar,⁶ A. Bean,⁷ J. Gronberg,⁷ R. Kutschke,⁷ S. Menary,⁷ R. J. Morrison,⁷ S. Nakanishi,⁷ H. N. Nelson,⁷ T. K. Nelson,⁷ J. D. Richman,⁷ A. Ryd,⁷ H. Tajima,⁷ D. Schmidt,⁷ D. Sperka,⁷ M. S. Witherell,⁷ M. Procaro,⁸ S. Yang,⁸ R. Balest,⁹ K. Cho,⁹ M. Daoudi,⁹ W. T. Ford,⁹ D. R. Johnson,⁹ K. Lingel,⁹ M. Lohner,⁹ P. Rankin,⁹ J. G. Smith,⁹ J. P. Alexander,¹⁰ C. Bebek,¹⁰ K. Berkelman,¹⁰ D. Besson,¹⁰ T. E. Browder,¹⁰ D. G. Cassel,¹⁰ H. A. Cho,¹⁰ D. M. Coffman,¹⁰ P. S. Drell,¹⁰ R. Ehrlich,¹⁰ M. Garcia-Sciveres,¹⁰ B. Geiser,¹⁰ B. Gittelman,¹⁰ S. W. Gray,¹⁰ D. L. Hartill,¹⁰ B. K. Heltsley,¹⁰ C. D. Jones,¹⁰ S. L. Jones,¹⁰ J. Kandaswamy,¹⁰ N. Katayama,¹⁰ P. C. Kim,¹⁰ D. L. Kreinick,¹⁰ G. S. Ludwig,¹⁰ J. Masui,¹⁰ J. Mevissen,¹⁰ N. B. Mistry,¹⁰ C. R. Ng,¹⁰ E. Nordberg,¹⁰ M. Ogg,^{10,*} J. R. Patterson,¹⁰ D. Peterson,¹⁰ D. Riley,¹⁰ S. Salman,¹⁰ M. Sapper,¹⁰ H. Worden,¹⁰ F. Würthwein,¹⁰ P. Avery,¹¹ A. Freyberger,¹¹ J. Rodriguez,¹¹ R. Stephens,¹¹ J. Yelton,¹¹ D. Cinabro,¹² S. Henderson,¹² K. Kinoshita,¹² T. Liu,¹² M. Saulnier,¹² F. Shen,¹² R. Wilson,¹² H. Yamamoto,¹² B. Ong,¹³ M. Selen,¹³ A. J. Sadoff,¹⁴ R. Ammar,¹⁵ S. Ball,¹⁵ P. Baringer,¹⁵ D. Coppage,¹⁵ N. Copty,¹⁵ R. Davis,¹⁵ N. Hancock,¹⁵ M. Kelly,¹⁵ N. Kwak,¹⁵ H. Lam,¹⁵ Y. Kubota,¹⁶ M. Lattery,¹⁶ J. K. Nelson,¹⁶ S. Patton,¹⁶ D. Perticone,¹⁶ R. Poling,¹⁶ V. Savinov,¹⁶ S. Schrenk,¹⁶ R. Wang,¹⁶ M. S. Alam,¹⁷ I. J. Kim,¹⁷ B. Nemati,¹⁷ J. J. O'Neill,¹⁷ H. Severini,¹⁷ C. R. Sun,¹⁷ M. M. Zoeller,¹⁷ G. Crawford,¹⁸ C. M. Daubenmier,¹⁸ R. Fulton,¹⁸ D. Fujino,¹⁸ K. K. Gan,¹⁸ K. Honscheid,¹⁸ H. Kagan,¹⁸ R. Kass,¹⁸ J. Lee,¹⁸ R. Malchow,¹⁸ F. Morrow,¹⁸ Y. Skovpen,^{18,†} M. Sung,¹⁸ C. White,¹⁸ J. Whitmore,¹⁸ P. Wilson,¹⁸ F. Butler,¹⁹ X. Fu,¹⁹ G. Kalbfleisch,¹⁹ M. Lambrecht,¹⁹ W. R. Ross,¹⁹ P. Skubic,¹⁹ J. Snow,¹⁹ P. L. Wang,¹⁹ M. Wood,¹⁹ D. Bortoletto,²⁰ D. N. Brown,²⁰ J. Fast,²⁰ R. L. McIlwain,²⁰ T. Miao,²⁰ D. H. Miller,²⁰ M. Modesitt,²⁰ S. F. Schaffner,²⁰ E. I. Shibata,²⁰ I. P. J. Shipsey,²⁰ and P. N. Wang²⁰

(CLEO Collaboration)

¹University of Rochester, Rochester, New York 14627

²Southern Methodist University, Dallas, Texas 75275

³Syracuse University, Syracuse, New York 13244

⁴Vanderbilt University, Nashville, Tennessee 37235

⁵California Institute of Technology, Pasadena, California 91125

⁶University of California, San Diego, La Jolla, California 92093

⁷University of California, Santa Barbara, California 93106

⁸Carnegie-Mellon University, Pittsburgh, Pennsylvania 15213

⁹University of Colorado, Boulder, Colorado 80309-0390

¹⁰Cornell University, Ithaca, New York 14853

¹¹University of Florida, Gainesville, Florida 32611

¹²Harvard University, Cambridge, Massachusetts 02138

¹³University of Illinois, Champaign-Urbana, Illinois 61801

¹⁴Ithaca College, Ithaca, New York 14850

¹⁵University of Kansas, Lawrence, Kansas 66045

¹⁶University of Minnesota, Minneapolis, Minnesota 55455

¹⁷State University of New York at Albany, Albany, New York 12222

¹⁸Ohio State University, Columbus, Ohio 43210

¹⁹University of Oklahoma, Norman, Oklahoma 73019

²⁰Purdue University, West Lafayette, Indiana 47907

(Received 11 August 1993)

We report results from a search for the decays $B^0 \rightarrow \pi^+\pi^-$, $B^0 \rightarrow K^+\pi^-$, and $B^0 \rightarrow K^+K^-$. We find 90% confidence level upper limits on the branching fractions, $B_{\pi\pi} < 2.9 \times 10^{-5}$, $B_{K\pi} < 2.6 \times 10^{-5}$, and $B_{KK} < 0.7 \times 10^{-5}$. While there is no statistically significant signal in the individual modes, the sum of $B_{\pi\pi}$ and $B_{K\pi}$ exceeds zero with a significance of more than 4 standard deviations, indicating that we have observed charmless hadronic B decays.

PACS numbers: 13.25.+m, 14.40.Jz

We have searched for the charmless decays $B^0 \rightarrow \pi^+\pi^-$, $B^0 \rightarrow K^+\pi^-$, and $B^0 \rightarrow K^+K^-$. The decay $B^0 \rightarrow \pi^+\pi^-$ involves a $b \rightarrow u$ spectator diagram and a possible contribution from a $b \rightarrow d$ penguin diagram (Fig. 1). This decay is of particular interest since the final state is a CP eigenstate and CP violation can arise from interference between the amplitude for the direct decay and that for the case where the B^0 mixes to a \bar{B}^0 and then decays [1]. The decay $B^0 \rightarrow K^+\pi^-$ is expected to occur via a $b \rightarrow s$ penguin diagram and a Cabibbo-suppressed $b \rightarrow u$ spectator diagram. Direct CP violation can result from interference between these diagrams [2].

While $b \rightarrow u$ transitions in the inclusive semileptonic mode $b \rightarrow u\ell\bar{\nu}$ are well established [3,4], and there is recent evidence for electromagnetic penguin decays ($b \rightarrow s\gamma$) in the exclusive channel $B \rightarrow K^*\gamma$ [5], there has been no confirmed indication of charmless hadronic B decays [6]. The most stringent published upper limits [7,8] are 9×10^{-5} for the branching fractions $B_{\pi\pi}$ and $B_{K\pi}$ for the $\pi^+\pi^-$ and $K^+\pi^-$ modes. We have updated a theoretical prediction [9] for $B_{\pi\pi}$ using the product $a_1|V_{cb}|\sqrt{\tau_{B^0}} = 0.054 \text{ ps}^{\frac{1}{2}}$, derived from measurements of two-body $b \rightarrow c$ decay modes in a recent review [10], and a new value $V_{ub}/V_{cb} = 0.08$ from CLEO [4]; the result is $B_{\pi\pi} = 1.1 \times 10^{-5}$. Recent theoretical predictions for $B_{K\pi}$ are in the range $(1-2) \times 10^{-5}$ [11]. The decay $B^0 \rightarrow K^+K^-$ is expected to be heavily suppressed since it involves both a $b \rightarrow u$ transition and W exchange.

We use data from the CLEO II detector [12] operating at the Cornell Electron Storage Ring (CESR). The sample consists of 1.37 fb^{-1} accumulated at a center-of-mass energy of 10.58 GeV on the $\Upsilon(4S)$ resonance, corresponding to 1.47×10^6 $B\bar{B}$ events. An additional sample of 0.64 fb^{-1} accumulated 55 MeV below the $\Upsilon(4S)$ provides a signal-free control sample. We refer to these as the “on-resonance” and “off-resonance” samples. The detector components important for this analysis are a tracking system consisting of a 6-layer straw tube chamber, a 10-layer vertex drift chamber, and a 51-layer main drift chamber, and an electromagnetic calorimeter consisting of 7800 CsI crystals, all operated inside a 1.5-T solenoidal magnet. The measured momentum resolution of the tracking system is given by $\sigma_p^2/p^2 = 0.0050^2 + 0.0015^2 p^2$ (p in GeV/c). We identify particles based upon specific ionization (dE/dx) information from the main drift chamber.

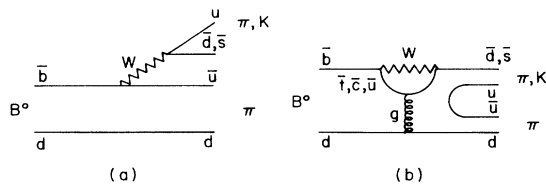


FIG. 1. (a) Spectator diagrams for $B^0 \rightarrow \pi^+\pi^-$ and $B^0 \rightarrow K^+\pi^-$ and (b) penguin diagrams for the same modes.

To search for $\pi^+\pi^-$, $K^+\pi^-$, and K^+K^- candidates, we select events with at least five charged tracks. Since B 's are produced nearly at rest, the two daughters will be nearly back-to-back, with momenta $\sim 2.6 \text{ GeV}/c$. We select two oppositely charged, well-measured candidate tracks which come from a common point consistent with the known event vertex, and for which the direction of the thrust axis lies within a fiducial volume defined by $|\cos\theta| \leq 0.8$, where θ is the polar angle with respect to the beam axis. We use the energies (E_1, E_2) calculated assuming both tracks are pions to compute the difference between their total energy and the beam energy, $\Delta E = E_1 + E_2 - E_b$. The ΔE distributions for $\pi\pi$, $K\pi$, and KK events are centered at 0, -42 , and -84 MeV, respectively. The resolution ($\sigma_{\Delta E}$) in ΔE is 25 ± 2 MeV [13]. We calculate a “beam-constrained” mass from $m^2 = E_b^2 - (\mathbf{p}_1 + \mathbf{p}_2)^2$ by using the constraint $\Delta E = 0$. The resolution in m , determined from fully reconstructed B decays, is 2.5 ± 0.2 MeV, 10 times smaller than without the beam constraint. We accept events lying in a fiducial region defined by $-185 < \Delta E < 140$ MeV and $5.210 < m < 5.289$ GeV, which includes the signal regions for $\pi\pi$, $K\pi$, and KK , and a sideband for background determination.

We differentiate between $\pi\pi$, $K\pi$, and KK events using ΔE and dE/dx information. The ΔE shift for $K\pi$ events provides a separation from $\pi\pi$ events of $1.7\sigma_{\Delta E}$. We have studied the dE/dx separation between pions and kaons for momenta $p \sim 2.6 \text{ GeV}/c$ using D^{*+} -tagged $D^0 \rightarrow K^-\pi^+$ decays; we find a separation of $(1.8 \pm 0.1)\sigma$.

We have studied backgrounds from $b \rightarrow c$ decays and other $b \rightarrow u$ and $b \rightarrow s$ decays and find that all are negligible in this analysis. The main background arises from the process $e^+e^- \rightarrow q\bar{q}$ (where $q = u, s, d, c$). Such events typically exhibit a two-jet structure and can produce high momentum, approximately back-to-back tracks in the fiducial region. To reduce contamination from these events, we calculate the angle, θ_T , between the thrust axis of the candidate tracks and the thrust axis of all the remaining charged and neutral energy in the event. The distribution of $\cos\theta_T$ is strongly peaked near ± 1 for $q\bar{q}$ events and is nearly flat for $B\bar{B}$ events. After requiring $|\cos\theta_T| \leq 0.7$ we obtain a sample of 262 (138) events in the on-resonance (off-resonance) data set for further analysis. We use a detailed Monte Carlo simulation to determine the overall signal efficiency to be $(38 \pm 3)\%$.

Additional discrimination between signal and $q\bar{q}$ background is provided by a Fisher discriminant technique [14]. The Fisher discriminant is a linear combination $\mathcal{F} \equiv \sum_{i=1}^N \alpha_i y_i$ where the coefficients, α , are chosen to maximize the separation in \mathcal{F} between Monte Carlo signal and background samples. The 11 inputs, y_i , are the direction of the candidate thrust axis, the flight direction of the candidate B meson, and nine variables which measure the momentum flow of showers and tracks from the rest of the event in nine angular bins, each of 10° , cen-

tered about the candidate's thrust axis. Figure 2 shows the distribution of \mathcal{F} for signal and background obtained from Monte Carlo events, with background data from off-resonance and sideband samples overlaid. Both signal and background distributions are well fitted by Gaussians whose means are separated by 1.5σ .

We use two approaches to evaluate the amount of signal in the data sample. In the first approach we cut on ΔE , m , \mathcal{F} , and dE/dx , count the number of events in the signal region, and compare to the background level extrapolated from the sideband region. For each event we use the dE/dx information to determine the most probable hypothesis among $\pi\pi$, $K\pi$, and KK . After requiring $\mathcal{F} \leq 0.52$, we define a 2σ signal region in ΔE and m . A sideband region is defined as the portion of the fiducial region with $m \leq 5.274$ GeV, including the off-resonance data. The net efficiency for signal events is 19%. This procedure yields 6 (56) $\pi\pi$ events in the signal (sideband) region. From a Monte Carlo simulation of the background we determine that the ratio of background populations in the sideband and signal regions is 40.3. In the absence of a signal the binomial probability to obtain 6 or more events in the signal region out of a total of 62 events is 3.9×10^{-3} . In the $K\pi$ mode there are 6 (56) events in the signal (sideband) region. From the sideband-signal ratio of 38.0, we find a binomial probability of 5.1×10^{-3} . There are 0 (38) KK events in the signal (sideband) region. For the combined $\pi\pi$ and $K\pi$ samples, with 12 (112) signal (sideband) events, the binomial probability that the observed sample results from a background fluctuation is 6.8×10^{-5} . Extrapolating to find the background in the signal region, we expect 1.4, 1.5, and 1.0 background events in $\pi\pi$, $K\pi$, and KK , respectively.

In the second approach, we increase the efficiency of

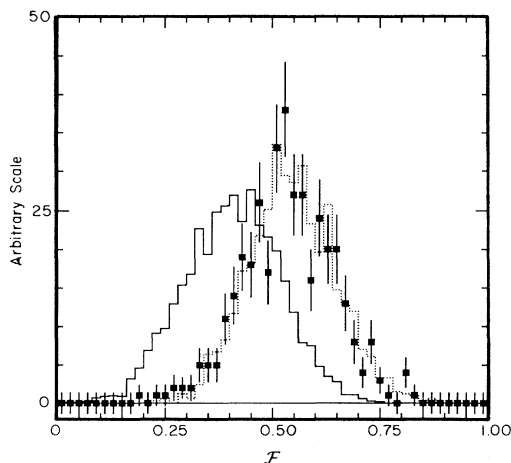


FIG. 2. Comparison of signal (solid histogram) and background (dashed histogram) Monte Carlo distributions for the Fisher variable \mathcal{F} . The points with error bars are from off-resonance plus sideband data.

the search and exploit the information contained in the shapes of the ΔE , m , \mathcal{F} , and dE/dx distributions, by releasing the cuts described in the previous paragraph and using these variables as inputs to an unbinned maximum-likelihood fit. In this fit the events in the fiducial region are parametrized by sums of probability density functions (PDF's) for $\pi\pi$, $K\pi$, and KK signal and background events, with relative areas determined by maximizing the likelihood function. The signal and background PDF's are Gaussian in all variables except background ΔE , which we parametrize with a low order polynomial, and background m , for which we use the empirical shape [8] $f(m) \propto m\sqrt{1-x^2} \exp[-\gamma(1-x^2)]$, with $x \equiv m/E_b$ and γ a parameter to be fit. The parameters of the PDF's are determined from high-statistics Monte Carlo samples. We use data to examine correlations among the input variables and find them to be small. Further details about this analysis and the likelihood fit in particular, can be found in Ref. [15].

The result of the maximum likelihood fit to the on-resonance data is given in Fig. 3. The figure shows a contour plot of $N_{K\pi}$ vs $N_{\pi\pi}$ in which the solid lines represent $n\sigma$ contours ($n=1-4$), corresponding to decreases in the log likelihood from its maximum by $0.5n^2$; the dotted line represents the 1.28σ contour which can be used to extract approximate 90% confidence level limits. The best fit values are $N_{KK} = 0.0_{-0.0}^{+0.8}$, $N_{\pi\pi} = 7.2_{-3.5}^{+4.3}$, and $N_{K\pi} = 6.4_{-3.1}^{+3.9}$, the latter two corresponding to excesses of 2.5σ and 2.8σ (statistical errors only). While neither the $\pi\pi$ nor the $K\pi$ excess is compelling, the point $N_{\pi\pi} = N_{K\pi} = 0$ is excluded at the level of 5.4σ . After simultaneously varying all parameters within their allowed range in the direction which decreases the summed signal, this point is still excluded at the 4.2σ level, indicating that either $\pi\pi$ or $K\pi$ or both are present in the data.

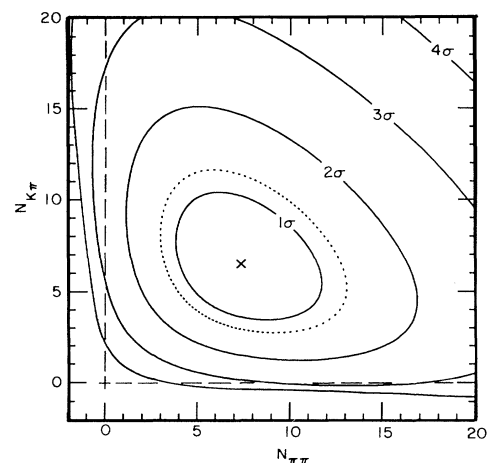


FIG. 3. Likelihood contours for the fit to $N_{\pi\pi}$ and $N_{K\pi}$. The central value of the fit is indicated by the cross. The solid lines are 1σ , 2σ , 3σ , 4σ contours and the dotted line is the 1.28σ contour.

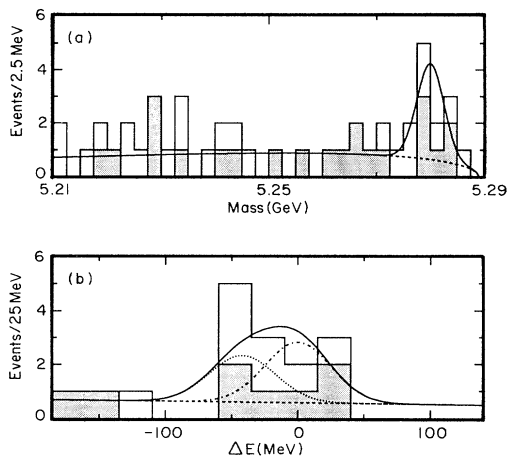


FIG. 4. Comparison of on-resonance data (histogram) with projections of the maximum likelihood fit (solid curve). (a) Sum of $K\pi$ and $\pi\pi$, projected onto m after cut on ΔE and \mathcal{F} ; (b) projection onto ΔE , after cut on m and \mathcal{F} . The shaded portions of the histograms indicate events identified as $\pi\pi$. In (b), the dotted and dot-dashed lines indicate the fit projections for $K\pi$ and $\pi\pi$ separately.

The results of the likelihood fit are checked in several ways. We fit the off-resonance data and find that the signals are consistent with zero as they should be: $N_{\pi\pi} = 0.7_{-0.7}^{+1.7}$ and $N_{K\pi} = 0.0_{-0.0}^{+0.6}$. We determine the confidence levels of the on- and off-resonance fits to be 35% and 74% by comparing the maximum value of the likelihood function for the actual data with that for 1000 simulated, 262-event or 138-event samples generated from the PDF's with the best fit values of the fitted parameters. This confirms that the PDF's accurately represent the data. In Fig. 4 we compare the maximum likelihood results with the event-counting analysis described earlier. To do this we project the maximum likelihood fit onto the m and ΔE axes and normalize by integrating over the remaining variables with the cuts used for the event counting analysis. We overlay these curves on the histograms of events identified in the event counting analysis as either $K\pi$ or $\pi\pi$ (note that the curves are not fits to these particular event histograms). The agreement between the curves and the histograms confirms the consistency of the two analyses.

Systematic uncertainties are estimated by varying the parameters of the PDF's for both signal and background within a range determined either from the off-resonance and sideband data or from independent measurements. Most variations shift events between $\pi\pi$ and $K\pi$ but change the sum very little. The sum is most sensitive to changes of the shape of $f(m)$, leading to 8% variations in the total yield. The individual yields of $\pi\pi$ and $K\pi$ are sensitive to $f(m)$, shifts in the zero of the ΔE distribution, and to the uncertainties in the dE/dx distributions. The total systematic errors of 9% for the sum and 16% for the individual yields are small compared to the statistical uncertainty.

TABLE I. Measured branching fractions and 90% C.L. upper limits (U.L.).

Mode	N_{fit}	B (10^{-5})	U.L. (10^{-5})
$\pi^+\pi^-$	$7.2_{-3.5}^{+4.3}$	$1.3_{-0.6}^{+0.8} \pm 0.2$	2.9
$K^+\pi^-$	$6.4_{-3.1}^{+3.9}$	$1.1_{-0.6}^{+0.7} \pm 0.2$	2.6
K^+K^-	$0.0_{-0.0}^{+0.8}$	$0.0_{-0.0}^{+0.2}$	0.7
$\pi^+\pi^-$ or $K^+\pi^-$	$13.6_{-3.9}^{+4.7}$	$2.4_{-0.7}^{+0.8} \pm 0.2$	

The central values and upper limits are summarized in Table I. The branching fractions are calculated from the efficiency and number of produced B 's given above. To calculate the number of B^0 's produced, we have assumed equal production rates for charged and neutral B mesons. In order to determine 90% confidence level (C.L.) limits, we integrate the likelihood function within the physical region. When systematic errors are added linearly, we find $B_{\pi\pi} < 2.9 \times 10^{-5}$, $B_{K\pi} < 2.6 \times 10^{-5}$, and $B_{KK} < 0.7 \times 10^{-5}$. These are significant improvements upon the previous limits of 9×10^{-5} [7], and for $B_{\pi\pi}$ and $B_{K\pi}$ are close to the level of the theoretical predictions [9,11]. While there is no statistically significant signal in any of the individual modes, the result for the sum, $B_{\pi\pi} + B_{K\pi}$, is more than 4 standard deviations from zero, indicating that we have observed charmless hadronic B decays.

We gratefully acknowledge the effort of the CESR staff in providing us with excellent luminosity and running conditions, and useful discussions with A. Silverman and D. Amidei. This work was supported by the National Science Foundation, the U.S. Department of Energy, the SSC Fellowship program of the TNRLC, the Heisenberg Foundation, and the A.P. Sloan Foundation.

* Permanent address: Carleton University, Ottawa, Canada K1S 5B6.

† Permanent address: INP, Novosibirsk, Russia.

- [1] I. Dunietyz, Ann. Phys. (N.Y.) **184**, 350 (1988); M. Gronau, Phys. Rev. Lett. **63**, 1451 (1989).
- [2] J. M. Gerard and W. S. Hou, Phys. Rev. D **43**, 2909 (1991); H. Simma, G. Eilam, and D. Wyler, Nucl. Phys. B **352**, 367 (1991).
- [3] R. Fulton *et al.*, Phys. Rev. Lett. **64**, 16 (1990); H. Albrecht *et al.*, Phys. Lett. B **234**, 409 (1990).
- [4] J. Bartelt *et al.*, Phys. Rev. Lett. (to be published); Cornell Report No. CLNS 93/1240, CLEO 93-15 (unpublished).
- [5] R. Ammar *et al.*, Phys. Rev. Lett. **71**, 674 (1993).
- [6] H. Albrecht *et al.*, Phys. Lett. B **209**, 119 (1988); C. Bebek *et al.*, Phys. Rev. Lett. **62**, 8 (1989); K. Schubert, *Heavy Quark Physics*, edited by P. S. Drell and D. Rubin (AIP, New York, 1989).
- [7] D. Bortoletto *et al.*, Phys. Rev. Lett. **62**, 2436 (1989); P. Avery *et al.*, Phys. Lett. B **223**, 470 (1989).
- [8] H. Albrecht *et al.*, Phys. Lett. B **241**, 278 (1990); H. Albrecht *et al.*, Phys. Lett. B **254**, 288 (1991).
- [9] M. Bauer, B. Stech, and M. Wirbel, Z. Phys. C **34**, 103 (1987).
- [10] M. Neubert, V. Rieckert, B. Stech, and Q. P. Xu, in

Heavy Flavors, edited by A. J. Buras and M. Lindner (World Scientific, Singapore, 1992). The symbols in the product are defined in this review.

- [11] N. G. Deshpande and J. Trampetic, *Phys. Rev. D* **41**, 895 (1990); L. L. Chau *et al.*, *Phys. Rev. D* **43**, 2176 (1991).
- [12] Y. Kubota *et al.*, *Nucl. Instrum. Methods Phys. Res., Sect. A* **320**, 66 (1992).
- [13] We use muon pairs to determine the momentum resolution at 5.3 GeV/c, and the decay modes $B \rightarrow \psi K$, $B \rightarrow D\pi$, and $B \rightarrow D^*\pi$ to determine the momentum resolution in the range 1.5–2.5 GeV/c.
- [14] R. A. Fisher, *Ann. Eugen.* **7**, 179 (1936); M. G. Kendall and A. Stuart, *The Advanced Theory of Statistics* (Hafner, New York, 1968), 2nd ed., Vol. III, Sec. 44.5ff.
- [15] J. P. Alexander *et al.*, Cornell Report No. CLNS 93/1252 (unpublished).